

# A kinetics model of hydrogen absorption and desorption in Ti-doped NaAlH<sub>4</sub>

Weifang Luo\*, Karl J. Gross

Analytical Material Science Department, Sandia National Laboratories, P.O. Box 969, Livermore, CA 94550, USA

Received 3 May 2004; received in revised form 13 May 2004; accepted 13 May 2004

## Abstract

The kinetics of the hydrogen sorption of Ti-doped direct-synthesized NaAlH<sub>4</sub> has been studied by measuring sorption rates at various temperatures and applied pressures. Formation and decomposition rate equations for NaAlH<sub>4</sub> and Na<sub>3</sub>AlH<sub>6</sub> are proposed, and pre-exponential factors and activation energies have been calculated for these reactions. These equations were used to calculate alanate decomposition curves. The results fit the experimental data very well. The predictive capabilities of this empirical approach provide a very useful modeling tool for optimizing the performance of the alanates over a range of hydrogen absorption temperatures and pressures. Under a typical hydrogen-loading condition (constant pressure), the optimum temperature for “fast fill” can be determined.

© 2004 Elsevier B.V. All rights reserved.

*Keywords:* Ti-doped; Kinetics; NaAlH<sub>4</sub>

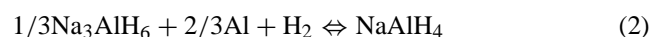
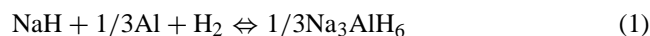
## 1. Introduction

The discovery that hydrogen can be easily absorbed and desorbed from Ti-doped sodium–aluminum hydrides (the alanates) has created an entirely new prospect for lightweight hydrogen storage [1]. These materials have nearly ideal equilibrium thermodynamics [1,2]. Doping the alanates with Ti and other transition metals enables the reverse (hydriding) reactions to take place under moderate conditions (<100 °C and <100 bar H<sub>2</sub>) [1,2]. However, sorption rates for this system remain a critical issue for vehicular hydrogen storage applications. Initial studies of alanate kinetics have focused on the dependence of the reaction rates on temperature [3]. The effect of Ti-doping on the reaction rates have also been measured [3]; however, the mechanism of enhanced kinetics is still not fully understood. The effect of hydrogen gas pressures and phase composition of reaction rates have not been evaluated until recently by Anton et al. [4].

Hydriding/dehydriding reaction kinetics has been well studied for interstitial hydrides [5–8]. These are multiple-step reactions, which include hydrogen transport in the gas-phase, hydrogen adsorption on the surface, hy-

drogen diffusion on the surface, H<sub>2</sub> dissociation on the surface, hydrogen absorption into the solid, hydrogen diffusion and hydride formation [5–8]. The dependence of the hydrogen sorption rate on temperature, hydrogen pressure and geometry of solids has been deduced using different models for the various rate-limiting steps [5–8].

The extensive work on the kinetics of interstitial hydrides provides a foundation for the study of hydriding kinetics in the alanates system. It is important, however, to recognize that the mechanism of hydrogen uptake and release is somewhat different for alanates than interstitial hydrides. In this case, sorption occurs through complex solid–solid and solid–gas phase formation and decomposition reactions. The formation and decomposition of the alanates Na<sub>3</sub>AlH<sub>6</sub> and NaAlH<sub>4</sub> are described by the following reactions



Unlike interstitial hydrides, these are stoichiometric compounds with no hydrogen solid solutions of either phase. The two reactions exhibit very different plateau pressures observed as discrete jump in pressure in the single Na<sub>3</sub>AlH<sub>6</sub> phase region [1].

The formation reactions involve more than one solid phase, which implies the existence of long-range diffusion of solid species aluminum or sodium [9,10].

\* Corresponding author. Tel.: +1-925-294-3729; fax: +1-925-294-3410.

E-mail address: wluo@sandia.gov (W. Luo).

### Nomenclature

$dC(H)/dt$	rate of concentration change of H in alanate formed (+) or decomposed (–), as H wt.%.
$E_{aa1}$	activation energy of NaAlH <sub>4</sub> formation
$E_{ad1}$	activation energy of NaAlH <sub>4</sub> decomposition
$E_{aa2}$	activation energy of Na <sub>3</sub> AlH <sub>6</sub> formation
$E_{ad2}$	activation energy of Na <sub>3</sub> AlH <sub>6</sub> decomposition
H wt.%	weight percent of H in sample
$K_0$	pre-exponential factor of rate constant
$K$	rate constant, $K = K_0 e^{(-E_{a1}/RT)}$
$P_{appl}$	applied pressure
$P_{eq1}$	plateau pressure of NaAlH <sub>4</sub> at a given temperature
$P_{eq2}$	plateau pressure of Na <sub>3</sub> AlH <sub>6</sub> at a given temperature

The mechanism of catalyst of Ti-containing compounds is not fully understood [11,12]. In previous studies, it was found that rates of hydrogen desorption are strongly dependent on temperature and the level of Ti-doping (between 1 and 6 mol.%) [3]. A detailed evaluation of desorption rates in terms of an exponential temperature dependence using the rate Eq. (3) provided a measure of the activation energy ( $E_a$ ) and a pre-exponential term ( $K$ ) for the decomposition of both alanate phases [3].

$$\text{Rate} = K \exp\left(-\frac{E_a}{RT}\right) \quad (3)$$

It was shown that only minor doping levels (1 mol.% TiCl<sub>3</sub>) were necessary to significantly reduce the activation energy of decomposition for both NaAlH<sub>4</sub> and Na<sub>3</sub>AlH<sub>6</sub>. However, the rates of decomposition did continue to increase as the level of TiCl<sub>3</sub> increased [3]. This increase was ascribed to the pre-exponential coefficient  $K$ .

In the present study, we measured the forward (absorption) and reverse (desorption) rates of both Eqs. (1) and (2) under varying temperature and pressure conditions. We used the data to evaluate a number of different empirical rate equations, including a pressure-dependent term. The rate equations that gave the best overall results were then used to determine the best fit to pre-exponential coefficients and activation energies. These values were used to predict kinetic behavior over a broad range of temperatures and pressures. Such a model should prove useful for optimizing operational conditions for real world hydrogen storage applications.

## 2. Experiment

### 2.1. Sample preparation

Samples were prepared using the direct synthesis method as described elsewhere [13]. Initial materials,

aluminum powder (~20 micron, 99+% Sigma–Aldrich), sodium hydride (Sigma–Aldrich) and solid titanium tri-chloride (Sigma–Aldrich) were weighed in molar ratio of NaH:Al:TiCl<sub>3</sub> = 112:100:4 in an argon-filled glove box. The excess NaH was added to compensate for the formation of NaCl [3]. The powders were mixed by ball milling under argon in a high-energy SPEX mill for 30 min. After mixing, a sample of about 3 g was transferred in the argon atmosphere glove box to a stainless steel reaction vessel. The sample holder had a thermocouple located in the center of the sample to monitor temperature in the reaction zone.

### 2.2. Experimental details

Sorption rates and hydrogen capacities were obtained volumetrically using a carefully calibrated Sieverts' apparatus. During sorption, the sample temperature, dosing volume temperature and applied pressure were monitored and recorded. Hydrogen pressures for absorptions were under 120 bar, and monitored using a transducer of Teledyne Taber model 206 piezoelectric, 0–200 bar with a resolution of 0.1 bar. Desorption pressures were monitored using a 0–3 bar Baratron capacitance manometer with resolution of 0.001 bar.

The sample was heated to 125 °C under vacuum for 20 min prior to being exposed to hydrogen. High purity hydrogen (Matheson Trigas research purity, 99.999%) was then introduced into the reaction vessel. The first absorption cycle was slow; however, the reaction rates increased with subsequent cycles. By the third cycle, the sample was activated and ready for sorption rate tests. During sorption rate tests, the sample temperature was set at several temperatures in steps between 60 °C and 180 °C for desorption, and 60 °C and 160 °C for absorption. All pressure and temperature data were acquired and recorded by computer using LabView-based software.

Before desorption measurements, the sample was heated to 125 °C and exposed to about 100 bar of hydrogen in order to completely hydride the sample. When the pressure in the chamber was stable (generally about 2 h), the hydriding process was completed and the sample was, then, cooled down to room temperature. Desorption rate measurement began at room temperature by opening the reaction vessel to a large calibrated volume (approximately 1.2 l) that had been evacuated. The temperature was increased gradually in steps, about 15–40 min for each step. The amount of hydrogen desorbed from the sample was determined from the pressure rise in the calibrated volume. Desorption rates were calculated in weight percent from the change in hydrogen pressure over a given time period. When a desorption-rate test was completed, the sample was evacuated at 160 °C for 2 h to completely desorb the sample; the sample was then ready for next absorption rate test.

The absorption rate measurements were performed in a similar manner to desorption rate measurements using a smaller calibrated volume of approximately 0.1 l. The

amount of hydrogen absorbed was measured at different temperatures, and the absorption rates were calculated in weight percent from the pressure drop over a given period of time.

### 3. Results and discussion

#### 3.1. Desorption measurements

A typical desorption measurement is shown in Fig. 1. The amount of desorbed hydrogen is given in terms of weight percentage of the total sample weight. The temperature was raised from room temperature and gradually increased to 180 °C. Hydrogen release became detectable starting at 60 °C. When the amount of hydrogen released from the sample approached 2.3 wt.%, the desorption rate dropped off. This indicates that 2.3 wt.% was the end of NaAlH<sub>4</sub> decomposition. The cause analysis for incomplete hydride formation will be discussed later in this paper. After the decomposition of NaAlH<sub>4</sub>, the temperature was reduced to 100 °C and kept at this temperature for 20 min. No hydrogen release was observed at 100 °C even after the applied hydrogen pressure was reduced to zero (by evacuation). Then the temperature was increased to 120 °C and

the Na<sub>3</sub>AlH<sub>6</sub> started to release hydrogen. The desorption rate increased as the temperature was raised in steps until the Na<sub>3</sub>AlH<sub>6</sub> decomposition was complete.

In desorbing, the reaction rate drops off in time. This is due to the combined action of the concentration of the desorbing phase approaching zero and the hydrogen over-pressure rising towards the equilibrium pressure. As the hydrogen pressure approaches the equilibrium pressure, the driving force for the reactions is lowered and the decomposition rate drops to zero at equilibrium. If the applied hydrogen pressure was higher than the equilibrium pressure, such as when temperature is suddenly lowered, instead of desorbing, the sample would begin to absorb hydrogen. Therefore, an analytical model of the rate behavior must necessarily include the relative concentration of reactants and the driving force. This is the motivation behind the empirical model we present here.

#### 3.2. Hydrogen capacity

Theoretical hydrogen capacity for alanate is 5.6 wt.%, i.e., 3.7 wt.% from Eq. (2) and 1.9 wt.% from Eq. (1). However, in this study the maximum H wt.% was about 3.9 wt.%; 2.23 wt.% comes from Eq. (2) and 1.67 wt.% from Eq. (1). This is due the following reasons:

- Hydrogen weight percentage was calculated based on total weight of the sample, including active and inactive components.
- The molar ratio of the sample was NaH:Al:TiCl<sub>3</sub> = 1.12:1:0.04. Here, the NaH molar ratio used was 1.12, instead of 1, because of the need to compensate for the loss of Na resulting from formation of NaCl [3]. NaCl formation, together with the weight of TiCl<sub>3</sub>, results in total inactive components as 15 wt.%.
- Chemically prepared and purified NaAlH<sub>4</sub> will release the full 5.6 wt.% hydrogen [1]. However, previous work by others showed that the NaAlH<sub>4</sub> formation as shown in Eq. (2) does not reach 100% completion; instead, it stops at about 75% completion in the temperature range of 150–200 °C [1]. This is probably due to the presence of “isolated islands” of reactant, the Na<sub>3</sub>AlH<sub>6</sub> and Al, after about 75% completion of NaAlH<sub>4</sub> formation [10]. XRD results for samples hydrided at 100 bar typically show that it is a mixture of NaAlH<sub>4</sub> and Na<sub>3</sub>AlH<sub>6</sub> with a molar ratio of approximately 2:1.

With these considerations, the maximum hydrogen weight percentage in the sample is 3.9 wt.%, the slightly less-than-theoretical hydrogen content for the Na<sub>3</sub>AlH<sub>6</sub> phase (1.67%) can be primarily accounted for by the weight of the inactive component TiCl<sub>3</sub>. Thus, the reactions consist of the full formation and decomposition of Na<sub>3</sub>AlH<sub>6</sub> for hydrogen weight percentage between 0 < H wt.% < 1.67%, and the partial formation and decomposition of NaAlH<sub>4</sub> for hydrogen concentrations between 1.67% < H wt.% < 3.9%.

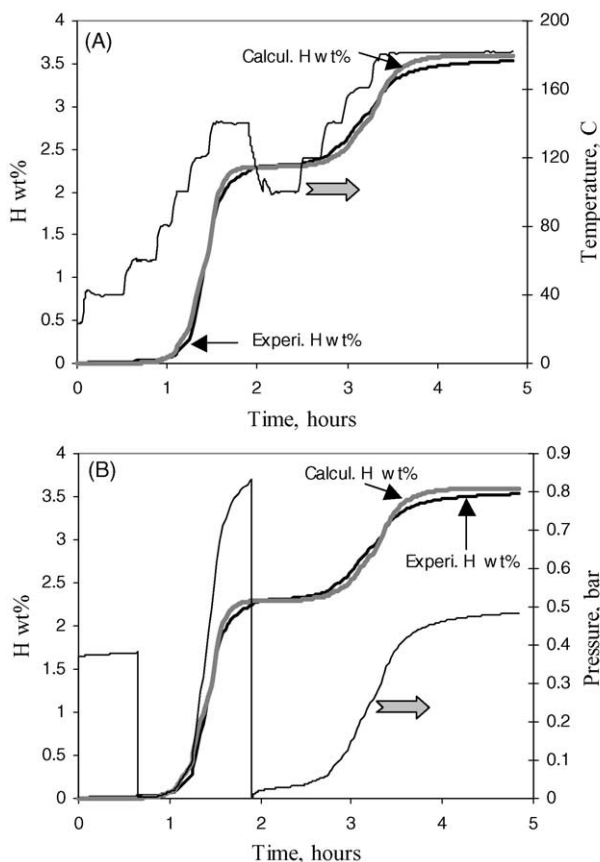


Fig. 1. NaAlH<sub>4</sub> and Na<sub>3</sub>AlH<sub>6</sub> decomposition profile at various temperatures (A) and pressures (B). Thick lines are for hydrogen wt.%, and thin lines for temperature (A) and hydrogen pressure (B), respectively.

### 3.3. Dependence of reaction rates on applied hydrogen pressure and reactant concentration at various temperatures

Ultimately, one would like to study kinetics in terms of the fundamental processes occurring during hydrogen absorption and desorption. Many models have been developed for hydrides to examine these processes and to aid in determining the rate-limiting mechanism [5–8]. However, to make mechanistic determinations for a particular hydride system based on such a kinetic analysis requires extremely well-defined experimental conditions, such as near-perfect isothermal conditions, and well-defined particle sizes and shapes. At this point, very little is actually known about how the alanate phase transitions even take place on an atomic scale. Thus, the purpose of this study was not to attempt to perform reaction rate analysis at a mechanistic level, but rather to find a set of empirical rate equations that accurately describe the hydrogen sorption behavior of the alanates on a performance level. The goal was to achieve a predictive model to aid in developing hydrogen storage systems and better materials.

To begin, the general sorption rate at a given temperature is a function of reactant concentration and applied pressure

$$d(\text{H wt.}\%)/dt = K_o \exp\left(-\frac{E_a}{RT}\right) * F(p) * F(\text{reactant concentrations}) \quad (3)$$

The term  $K_o \exp(-E_a/RT)$  is the rate constant, which is a function of temperature.  $K_o$  is a pre-exponential factor and  $E_a$  is the activation energy. We use the difference of logarithms of applied pressure and plateau pressure for the functional dependence of reaction rates on pressure. Thus, for both reactions 1 and 2, the rate dependence on hydrogen pressure is  $\ln(P_{\text{appl}}/P_{\text{eq}})$  for hydride formation and  $\ln(P_{\text{eq}}/P_{\text{appl}})$  for hydride decomposition.

The reason for using the logarithm of pressure will be discussed later in this paper.

As a first approximation, reactions (1) and (2) are considered to be independent reactions that take place one after the other. This is justified for alanates because far from equilibrium, the reaction rates are at least an order of magnitude slower for reaction 1 than reaction 2 for desorption and faster for absorption at a given temperature and pressure. We reported earlier on the serial behavior of the reactions for decomposition [9]. Recently, Gao et al. reported that they have found that these two reactions also take place sequentially on hydrogen absorption [13]. In order to simplify the calculation, the concentrations of reactants, such as Al, NaH, NaAlH<sub>4</sub> and Na<sub>3</sub>AlH<sub>6</sub>, can be replaced by H wt.%. This is because hydrogen is evolved or consumed in both reactions, and so by material balance in this system, the concentration of the solid phases are functions of the hydrogen weight-percent.

For Na<sub>3</sub>AlH<sub>6</sub> formation, there are two solid reactants, NaH and Al. Since there is an excess amount of Al, only the

NaH content is considered. Therefore, the rate of Na<sub>3</sub>AlH<sub>6</sub> formation is taken as first order of the NaH content (thus first order in H content). For NaAlH<sub>4</sub> formation, there is no excess amount of Al in the system. The concentration of both Na<sub>3</sub>AlH<sub>6</sub> and Al should be considered for this reaction. Therefore, the rate of NaAlH<sub>4</sub> formation is taken to be second order of the reactant contents (thus second order in H concentration). By contrast, decomposition rates for both reactions are taken as first order because only one solid reactant (NaAlH<sub>4</sub> or Na<sub>3</sub>AlH<sub>6</sub>) is involved in each reaction.

Based on the above principles, the rate equations for formation/decomposition for NaAlH<sub>4</sub> and Na<sub>3</sub>AlH<sub>6</sub> can be described as given in Eqs. (4)–(7). Note that reactant contents in these equations are now expressed as H wt.% in order to simplify the calculation, and the pressure considered here is within the range for hydrogen storage – about 0.1–150 bar.

- For NaAlH<sub>4</sub> formation:

$$d(\text{H wt.}\%)/dt = K_{oa1} \exp\left(-\frac{E_{aa1}}{RT}\right) \ln\left(\frac{P_{\text{appl}}}{P_{\text{eq1}}}\right) \times (3.9 - \text{H wt.}\%)^2; (1.67 < \text{H wt.}\% < 3.9) \quad (4)$$

- For NaAlH<sub>4</sub> decomposition:

$$-d(\text{H wt.}\%)/dt = K_{od1} \exp\left(-\frac{E_{ad1}}{RT}\right) \ln\left(\frac{P_{\text{eq1}}}{P_{\text{appl}}}\right) \times (\text{H wt.}\% - 1.67); (1.67 < \text{H wt.}\% < 3.9) \quad (5)$$

- For Na<sub>3</sub>AlH<sub>6</sub> formation:

$$d(\text{H wt.}\%)/dt = K_{oa2} \exp\left(-\frac{E_{aa2}}{RT}\right) \ln\left(\frac{P_{\text{appl}}}{P_{\text{eq2}}}\right) \times (1.67 - \text{H wt.}\%); (\text{H wt.}\% < 1.67) \quad (6)$$

- For Na<sub>3</sub>AlH<sub>6</sub> decomposition:

$$-d(\text{H wt.}\%)/dt = K_{od2} \exp\left(-\frac{E_{ad2}}{RT}\right) \ln\left(\frac{P_{\text{eq2}}}{P_{\text{appl}}}\right) \times (\text{H wt.}\%); (\text{H wt.}\% < 1.67) \quad (7)$$

The equilibrium plateau pressure ( $P_{\text{eq}}$ ) values used here for reactions 1 and 2 are taken from literature [9,14,15]. There are some indications that materials prepared by direct synthesis may have a more sloping character, and this of course would affect the analysis to at least a small degree [16], but this is not included in this model.

According to Eqs. (4)–(7), there should be straight lines on the plots of  $(-d(\text{H wt.}\%)/dt)$  versus  $(\ln(P_{\text{eq}}/P_{\text{appl}}) * (\text{H wt.}\%))$  for formation and  $(\ln(P_{\text{appl}}/P_{\text{eq}}) * (\text{H wt.}\%))$  for decomposition at constant temperature. It can be seen from the linear behavior at each temperature that this model fits well. The slopes of these lines are the rate constants  $K_o$



Table 1  
Summary of formation and decomposition activation energy of NaAlH<sub>4</sub> and Na<sub>3</sub>AlH<sub>6</sub>

	$K_o$ (abs)	$E_{aa}$ (abs) (kJ/mol)	$K_o$ (des)	$E_{ad}$ (des) (kJ/mol)	$E_{ad}$ (des) [3] (kJ/mol)
NaAlH <sub>4</sub>	$6.25 \times 10^8$	61.6	$1.9 \times 10^{11}$	85.6	80.0
Na <sub>3</sub> AlH <sub>6</sub>	$1.02 \times 10^8$	56.2	$2.9 \times 10^{10}$	88.3	97.5

be determined from these two figures, and the results are listed in Table 1.

The activation energy for decomposition of NaAlH<sub>4</sub> and Na<sub>3</sub>AlH<sub>6</sub> reported by Sandrock et al. [3] are listed for comparison.

### 3.5. Desorption simulations

To test our model, the rate Eqs. (4)–(7) were used to calculate the decomposition curves of NaAlH<sub>4</sub> and Na<sub>3</sub>AlH<sub>6</sub> from temperature and pressure data. The results of these simulations are presented in Fig. 1, along with the actual experimental data for comparison. It can be seen that the set of relationships that we determined to best represent these complex reactions (Eqs. (4)–(7)) provide a very reasonable means for modeling desorption behavior of the alanates over a broad range of conditions. This provides confidence that these relationships can be used in a predictive manner to optimize the alanate sorption processes for applications under various operating conditions.

### 3.6. Applications of the rate equations

Expanding on these simulations, we now present three examples of the predictive capabilities of these empirical relationships. This provides some insight into how this model can be applied as a powerful tool for optimizing performance in alanate hydrogen storage applications.

#### 3.6.1. Optimizing temperature and pressure for hydrogen absorption in forming NaAlH<sub>4</sub>

Temperature increase has two effects on a reaction rate: it increases both rate constants and plateau pressures. For hydride decomposition at a given applied pressure, both these effects lead to rate increase and, therefore, these effects reinforce each other so that desorption rates always increase by raising the temperature. For hydride formation, however, it is not the case. Temperature increase will increase rate constant, but also increases plateau pressure; that leads to rate reduction according to Eqs. (4) and (6). Thus, the net effect of temperature increase on absorption rate at a given applied pressure is not necessarily positive. This counteracting phenomenon has been reported for the alanates by the observation of higher absorption rate at 50 °C than at 70 °C for a given applied pressure [17].

This pressure versus temperature effect can be evaluated using the proposed absorption rate Eqs. (4) and (6). Rate constant  $K = K_o e^{(-E_{a1}/RT)}$  increases monotonically with temperature. However, the pressure driving force,  $\ln(P_{\text{appl}}/P_{\text{eq}})$ ,

decreases with increasing temperature for NaAlH<sub>4</sub> formation due to the higher  $P_{\text{eq}}$  at higher temperature. The net effect on rate due to increasing temperature can be positive or negative. For example, using  $K_o = 6.25 \times 10^8$ ;  $E_a = 61.6$  kJ/mol and assuming reactant concentration is a constant as H wt.% = 2.9%, the rate equation for NaAlH<sub>4</sub> formation, Eq. (4), becomes

$$d(\text{H wt.}\%)/dt = 6.25 \times 10^8 e^{(-7.4/T)} \ln\left(\frac{P_{\text{appl}}}{P_{\text{eq}}}\right) \quad (8)$$

Using these values, the calculated rates from 60 to 160 °C at applied pressure between 10 and 120 bar for NaAlH<sub>4</sub> formation are shown in Fig. 5. As an example of the counteracting effects of pressure and temperature, it can be seen from Fig. 6 that the absorption rate at 140 °C is higher than at 160 °C, when applied pressure is below 110 bar.

#### 3.6.2. Calculated formation rates for Na<sub>3</sub>AlH<sub>6</sub>

The formation rates for Na<sub>3</sub>AlH<sub>6</sub> can be calculated using the same approach as for NaAlH<sub>4</sub>. Unlike the NaAlH<sub>4</sub> case, however, the crossover of the absorption rates with temperature occurs at pressures below those commonly applied to these samples. For example, the plateau pressure for Na<sub>3</sub>AlH<sub>6</sub> at temperatures below 160 °C is below 7 bar, which is lower than applied pressure generally used for the charging process. Thus, for Na<sub>3</sub>AlH<sub>6</sub>, absorption rates typically increase with increasing temperature. Fig. 6 shows the calculated formation rates at various temperatures and

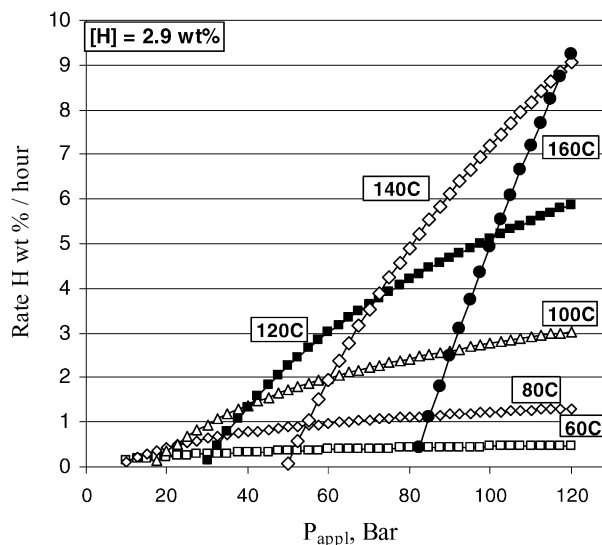


Fig. 5. Calculated formation rates of NaAlH<sub>4</sub> at several temperatures and applied pressures.

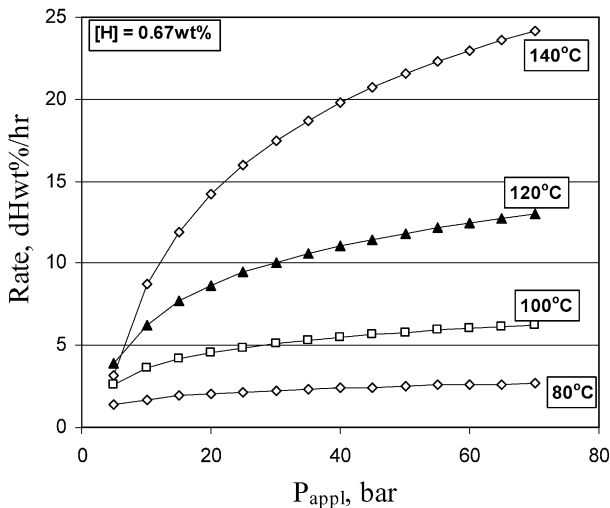


Fig. 6. Calculated formation rates for  $\text{Na}_3\text{AlH}_6$  at selected temperatures and applied pressures.

applied pressures. It can be seen that at applied pressure of 40 bar, the formation rate at hydrogen content of 0.67 wt.% is 11 wt.%/h at 120 °C and 20 wt.%/h at 140 °C.

### 3.6.3. Calculated decomposition rates for $\text{Na}_3\text{AlH}_6$ and $\text{NaAlH}_4$

Unlike hydride formation, the decomposition rates for both  $\text{Na}_3\text{AlH}_6$  and  $\text{NaAlH}_4$  increase with temperature regardless of the pressure, because both the rate constant  $K$  and decomposition driving force ( $P_{\text{eq}}/P_{\text{appl}}$ ) increase with temperature. To evaluate the influence of temperature on the hydrogen desorption rates, Eqs. (5) and (7) can be rewritten using the values of activation energy and pre-exponential factor listed in Table 1, and assuming values of H wt.% = 1% for  $\text{Na}_3\text{AlH}_6$  and H wt.% = 3.2% for  $\text{NaAlH}_4$ , which are close to the median hydrogen content in each plateau region.

For  $\text{NaAlH}_4$ :

$$-d(\text{H wt.})/dt = 1.9 \times 10^{11} e^{(-10.29/T)} \ln \left( \frac{P_{\text{eq}1}}{P_{\text{appl}}} \right) \quad (9)$$

For  $\text{Na}_3\text{AlH}_6$ :

$$-d(\text{H wt.})/dt = 2.9 \times 10^{10} e^{(-10.62/T)} \ln \left( \frac{P_{\text{eq}2}}{P_{\text{appl}}} \right) \quad (10)$$

We used  $P_{\text{eq}}$  values calculated from the van't Hoff plot [14,15] for Eqs. (9) and (10) to calculate decomposition rates for  $\text{Na}_3\text{AlH}_6$  and  $\text{NaAlH}_4$ . The results are plotted in Fig. 7. The vertical line at pressure of 1 bar is shown in this figure to indicate the decomposition rates at 1 bar. This provides a gauge for evaluating desorption rates for applications that typically require hydrogen supplied at near ambient conditions, such as fuel cells.

It can be seen from this figure that:

- it is possible to estimate discharge rates for the desorption reaction at over a broad range of pressures and temperatures;

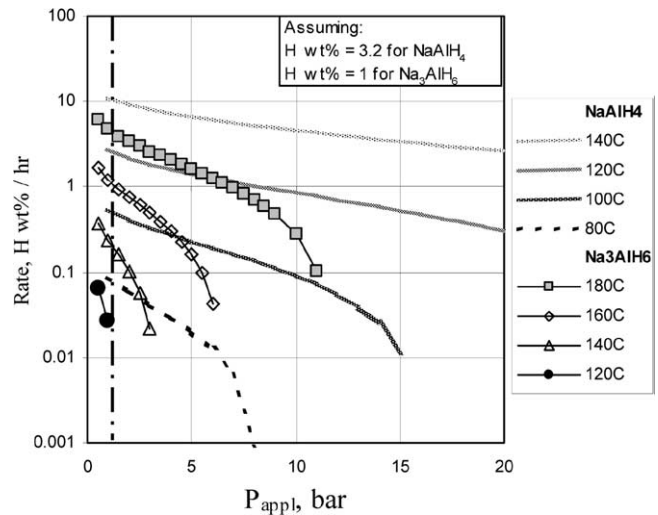


Fig. 7. Calculated decomposition rates of  $\text{NaAlH}_4$  and  $\text{Na}_3\text{AlH}_6$  over a typical range of applied pressures and temperatures for H wt.% = 3.2 ( $\text{NaAlH}_4$ ) and H wt.% = 1 ( $\text{Na}_3\text{AlH}_6$ ).

- at 120 °C and an applied pressure of 1 bar, the  $\text{Na}_3\text{AlH}_6$  decomposition rate is very low, about 0.07 H wt.%/h, compared to the decomposition rate of  $\text{NaAlH}_4$  which is 1.5 wt.%/h at the same temperature;
- at applied pressure of 1 bar, the decomposition rate for  $\text{Na}_3\text{AlH}_6$  becomes more significant when temperature is increased to 160 °C.

## 4. Conclusion

The kinetics of hydrogen absorption and desorption of Ti-doped direct-synthesized  $\text{NaAlH}_4$  was studied by measuring sorption rates over a wide range of temperatures and applied pressures. From these measurements, a series of formation and decomposition rate equations for  $\text{NaAlH}_4$  and  $\text{Na}_3\text{AlH}_6$  were determined. Using these rate equations, the pre-exponential rate constants and activation energies were calculated for the decomposition and reformation of these two alanate compounds. The calculated alanate decomposition curves using these empirical rate equations were tested and fit the experimentally measured results quite well. The kinetic performance of the alanate reactions can be predicted using these equations for a wide range of pressures and temperatures. As a result, it is possible to optimize alanate formation rates for any given pressure by selecting a proper temperature. For the  $\text{NaAlH}_4$  formation reaction at a fixed pressure, it is not always advantageous to increase the temperature to achieve the highest rate. This model provides a method for evaluating and optimizing the performance of alanates for a variety of hydrogen storage applications.

## Acknowledgements

The authors thank S. Spangler and K. Stewart for preparing samples and test equipment. This work is financially

supported by U.S. DOE under DE-AC04-94 AL 8500 and Sandia's Laboratory Directed Research and Development Project Office.

## References

- [1] B. Bogdanovic, R.A. Brand, A. Marjanovic, M. Schwickardi, J. Tolle, *J. Alloys Comp.* 302 (2000) 36–58.
- [2] C.M. Jensen, K.J. Gross, *Appl. Phys. A* 72 (2001) 213–219.
- [3] G. Sandrock, K. Gross, G. Thomas, *J. Alloys Comp.* 339 (2002) 299–308.
- [4] D.L. Anton, D.A. Mosher, S.M. Opalka, Hydrogen, Fuel Cells and Infrastructure Technologies Program Annual Merit Review Meeting, Berkeley, CA, May 19–22, 2003.
- [5] M.H. Mintz, J. Bloch, *Prog. Solid State Chem.* 16 (1985) 163–194.
- [6] T.B. Flanagan, in: A.F. Anderson, A.J. Maeland (Eds.), *Hydrides for Energy Storage*, Pergamon, Oxford, 1978, pp. 135–150.
- [7] P.D. Goodell, P.S. Rudman, *J. Less-Common Metals* 89 (1983) 117–125.
- [8] X.L. Wang, S. Suda, *Int. Hydrogen Energy* 17 (2) (1992) 139–147.
- [9] K.J. Gross, S. Guthrie, G.J. Thomas, *J. Alloys Comp.* 297 (1999) 270–281.
- [10] B. Bogdanovic, M. Felderhoff, M. Germann, M. Hartel, A. Pommerin, F. Schuth, C. Weidenthaler, B. Zibroius, *J. Alloys Comp.* 350 (2003) 246–255.
- [11] D. Sun, T. Kiyobayashi, H.T. Takishita, N. Kutiyama, C.M. Jensen, *J. Alloys Comp.* 337 (2002) L8–L11.
- [12] E.H. Majzoub, K.J. Gross, *J. Alloys Comp.* 356–357 (2003) 363–367.
- [13] K.J. Gross, E. Majzoub, G.J. Thomas, G. Sandrock, DOE Annual Review, 2002.
- [14] Y. Gao, J. Rijssenbeek, W. Heward, V. Smentkowski, Presentation at American Physics Society, Montreal, Canada, March 22–24, 2004.
- [15] K. Gross, G. Thomas, C. Jensen, *J. Alloys Comp.* 330–332 (2002) 683–690.
- [16] K.J. Gross, DOE Hydrogen and Fuel Cell Program Annual Review, 2003.
- [17] K.J. Gross, G. Sandrock, G.J. Thomas, *J. Alloys Comp.* 330–332 (2002) 691–695.